

# Orthogonal Frequency Division Multiplexing for Indoor Optical Wireless Communications using Visible Light LEDs

S. K. Hashemi<sup>1</sup>, Z. Ghassemlooy<sup>1</sup>, L. Chao<sup>2</sup>, and D. Benhaddou<sup>3</sup>

<sup>1</sup>*Optical Communications Research Group, NCRLab Northumbria University, Newcastle upon Tyne, UK*

<sup>2</sup>*Department of Electronic and Information Engineering, Hong Kong Polytechnic University*

<sup>3</sup>*Engineering Technology Department, College of Technology, University of Houston, USA*

*E-mail:*

[seyyedkamal.hashemi@unn.ac.uk](mailto:seyyedkamal.hashemi@unn.ac.uk), [fary.ghassemlooy@unn.ac.uk](mailto:fary.ghassemlooy@unn.ac.uk), [enluchao@polyu.edu.hk](mailto:enluchao@polyu.edu.hk), [dbenhaddou@uh.edu](mailto:dbenhaddou@uh.edu)

**Abstract**—Visible light LEDs are being used for indoor optical wireless systems as well as room lighting. In indoor diffuse optical wireless links multipath dispersion limits the maximum transmission data rates. In this paper we investigate OFDM system where multipath induced intersymbol interference (ISI) is reduced, enabling higher data rates. Pilot signals are uniformly inserted into data symbols (subcarriers) and are extracted at the receiver for channel estimation. Predicted and simulated results for the symbol error rate (SER) for an OFDM employing BPSK, QPSK and M-QAM for line of sight (LOS) and diffuse links are presented for a range of pilot signal.

## I. INTRODUCTION

The demand for a wireless broadband communication link capable of supporting multimedia applications at high data rates is growing. The existing RF and wired based technologies available (such as Wi-Fi, WiMax and WLAN) suffer from the bandwidth bottleneck but offer mobility and flexibility. In number of applications where higher data throughputs is more of requirement than the mobility, transmission link based on optical wireless would be one of the best options as outlined in [1-4]. Recently, white LEDs have been used for both illumination and indoor wireless communications [1-4]. Limited mobility can be provided using a diffuse optical wireless link but at the cost of the much reduced data rate due to multipath dispersion that gives rise to intersymbol interference (ISI) in high-speed systems. For a particular IR systems, the degree of multipath is complex to predict, and depends on many parameters such as room geometry, materials, the position of the transmitter, receiver and objects within the room, and system design.

A number of techniques have been proposed to combat ISI. In [5] guard slots are inserted into each differential pulse interval modulation scheme, whereas in [6] spread spectrum technique has been used to combat ISI but at the expense of reduced bandwidth efficiency. Angle diversity scheme based on multibeam-narrow FOV transceiver has also been employed to overcome multipath dispersion since a small fraction of the delayed light normally lies within the same field-of-view (FOV)

as the primary signal as in [7]. In [8] an adaptive decision equalizer is used to combat ISI. OFDM has been used in mainly RF based wireless communication schemes offering high data rates capability as well as high bandwidth efficiency and effectively dealing with the multipath induced ISI [9] and has been proposed in optical wireless communications by researchers [10]. In OFDM a large number of closely-spaced orthogonal subcarriers, each modulated at a low symbol rate, is employed to offer overall data rates similar to conventional single-carrier modulation schemes within the same channel bandwidth [9]. Since the duration of each symbol is long compared with the channel multipath time-spreading, then by inserting a guard slot between the symbols, it is feasible to eliminate the ISI. The guard slot is much shorter than the symbol length but longer than the channel multipath time-spreading. In this paper we investigate OFDM system where multipath induced ISI and the effects of background noise are reduced by taking the advantage of narrowband frequency interference, which affects only one of the frequency subbands when compare to the single-carrier modulation. This paper is organized as follows. In section 2, we introduced the proposed optical OFDM system, whereas in section 3 channel estimation details are given. Performance analysis and simulation are outlined in section 4, and finally concluding remarks are presented in section 5.

## II. OPTICAL OFDM

The Baseband model of an optical OFDM transmission system is depicted in Fig. 1. An input binary bit stream  $b[i]$  is grouped by passed through a serial-to-parallel (S/P) converter to generate parallel streams before being modulated. Here the modulation schemes adopted are the BPSK, QPSK, and M-QAM. The modulated output symbols are defined as  $X_d = \{X_0, X_1, \dots, X_{N_d-1}\}$ . Pilot signals (tones) are uniformly inserted into all symbols (sub-carriers) for channel estimation in diffuse links. For LOS links there are no pilot signals. The Inverse Fast Fourier Transform (IFFT) block is used to implement the OFDM, which to

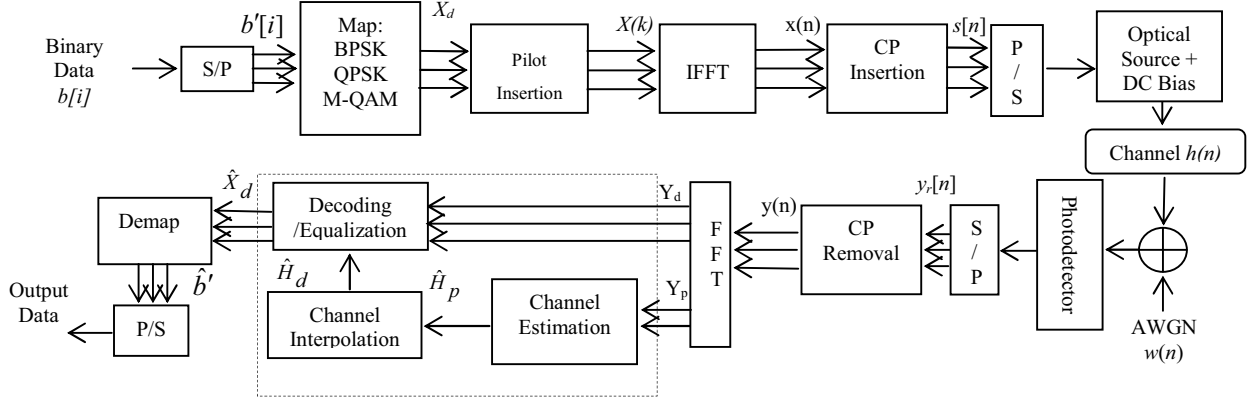


Fig 1. Baseband model of an optical OFDM system.

transform the data sequence  $X(k)$  of length  $N$  into a complex time-domain signal. The transmitted information symbols  $X(k)$  are the frequency coefficients and the output of the IFFT stage  $x(n)$  is the time domain of the input samples:  $x(n) = IFFT_N\{X(k)\}(n)$ , where  $n$  and  $k = 0, 1, 2, \dots, N-1$ . In optical system with intensity modulation, only real-value and positive signals are used, therefore in OFDM, the subcarriers should have Hermitian symmetry to produce real value. To mitigate the effects of multipath induced ISI, OFDM symbol is preceded by a guard interval of  $G$ -sample (or cyclic prefix (CP) as shown in Fig. 2 The length of  $G$ -sample depends on the channel delay spread and is normally considered to be greater than or equal to the channel length (impulse response time) to ensure prevent ISI [9].

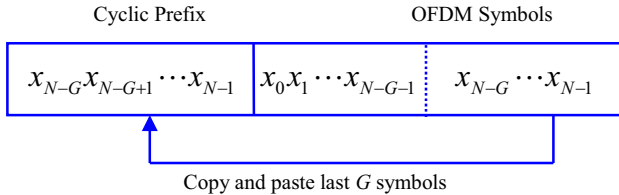


Fig 2. OFDM symbol structure with a cyclic prefix.

In optical transmission with Intensity Modulation/Direct Detection (IM/DD), a DC bias is usually added to the signal to ensure that the signals are all positive [10]. Finally, the OFDM signal is passed through a parallel-to-serial converter (P/S) to generate a discrete-time OFDM symbol  $s(n)$  of duration  $T_s = NT + GT$ , where  $\Delta f = B/N$  is the frequency spacing between the subcarriers within the bandwidth  $B$ , prior to being applied to the optical source.

The received OFDM signal propagated through the channel  $h(n)$  is given by:

$$y_r[n] = \Re.s[n] \otimes h[n] + w[n] \quad (1)$$

where  $w[n]$  is the additive white Gaussian noise

(AWGN),  $\Re$  is the photodetector responsivity, and  $\otimes$  denotes the circular convolution.

As for the channel impulse response, Barry [11] proposed a recursive algorithm to take into account higher order reflections, whereas in [12] a MIMO method for speedy calculation of the impulse response is presented. In [13,14] a Mont Carlo ray-tracing algorithm and its modified version uses both the Lambert's diffuse and the Phong's models to approximate surfaces with a strong specular component. A detailed derivation of the impulse response for the Sphere model was given in [15] and was practically measured by using the Ulbricht's integrating sphere in [16]. In [17] a fast iterative model capable of calculating high-order reflections is outlined. Due to the CP, the discrete linear convolution of  $s[n]$  and  $h[n]$  becomes a circular convolution hence simplifying the equalization process at the receiver. Thus at the receiver, the signal is passed through S/P and its CP from each received symbol is removed before being applied to the  $N$ -point FFT module for the following operation:

$$Y(k) = FFT_N\{y(n)\}, \quad (2)$$

where  $k = 0, 1, 2, \dots, N - 1$

### III. CHANNEL ESTIMATION

In OFDM system due to multi-amplitude modulation schemes, channel estimation is required for equalization and decoding provided there is no knowledge of the channel. In one dimensional channel estimation schemes pilot insertion could be done in (i) block-type and (ii) comb-type. The former uses the least square (LS) or the minimum mean-square error (MMSE) to perform estimation in a slow fading channel [18], whereas the latter uses the LS with interpolation and the maximum likelihood (ML) to perform estimation in a rapidly changing channel [19]. Here, we have adopted the latter for the indoor optical wireless channel. In the comb-type pilot based channel arrangement,  $N_p$  pilot symbols  $X_p = \{X_p(0), X_p(1), \dots, X_p(N_p - 1)\}$  are uniformly inserted into  $X_d$  according to the following expression:

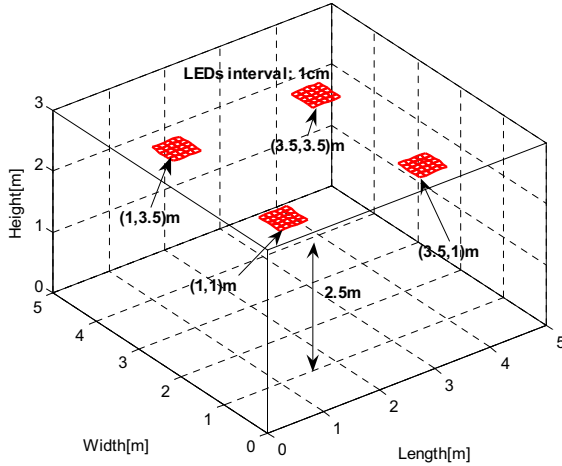


Fig 3. Positions of LEDs within a room with a size  $5 \times 5 \times 3m^3$

$\{X_p(0), X_d(0) \dots X_d(\text{Floor}(N_d / N_p) - 1), X_p(1), X_d(\text{Floor}(N_d / N_p)), \dots\}$  before performing IFFT.

Information on the exact locations of the pilot and data symbols as well as the values of the pilot symbols are already available at the receiver. The received pilot symbols  $Y_p$  are extracted from the received OFDM signal after the FFT block for channel estimation. The estimated channel  $\hat{H}_p$  at pilot subcarriers for the LS estimation (where there is no need for the prior knowledge of the variance of the noise) is given as:

$$\hat{H}_p(m) = \frac{Y_p(m)}{X_p(m)} \quad m = 0, 1, \dots, N_p - 1 \quad (3)$$

There are a number of interpolation schemes including the linear interpolation, the second-order interpolation, the spline cubic interpolation and the time domain interpolation which are used in the one dimensional model to extract channel information on the data subcarriers  $H_d$  [18]. In [21, 23] detailed information on the number of pilots used and how to locate them as optimal pilot design techniques are given.

#### IV. PERFORMANCE ANALYSIS AND SIMULATION

The proposed scheme is simulated with the following conditions. Optical sources used are four sets of white light LEDs located at a height of 2.5 m from the floor as shown in Fig. 3. We assumed the user terminal is at a desk height of 85 cm. Both LOS and diffuse links are considered. The properties of photometric and radiometric are employed for the distribution of luminous intensity. The radiation pattern is assumed to be Lambertian with the order of semi-angle half illuminance of an LED equal to  $n = -\ln 2 / \ln(\cos(\phi_{1/2}))$  at 70 degree and the following distribution:

$$R(\phi) = \frac{n+1}{2\pi} P_s \cdot \cos^n(\phi) \quad \text{for } \phi \in [-\pi/2, \pi/2] \quad (4)$$

where  $n$  is the Lambert's order expressing directivity of

Table I. Simulation parameters

Parameters	Values
Transmitted optical power $P_s$	20.0 mW
Centre luminance intensity of LED	730 mcd
Field of view (FOV)	60 Degree
Photodetector surface area $A_r$	1 cm <sup>2</sup>
Lambert mode	0.6461
Refractive index of the concentrator $n_r$	1.5
Photodetector responsivity	0.53 (A/W)
FFT size	256
Number of data subcarriers	128
Number of pilots	16,32,64
Cyclic prefix (CP) ratio	1/4

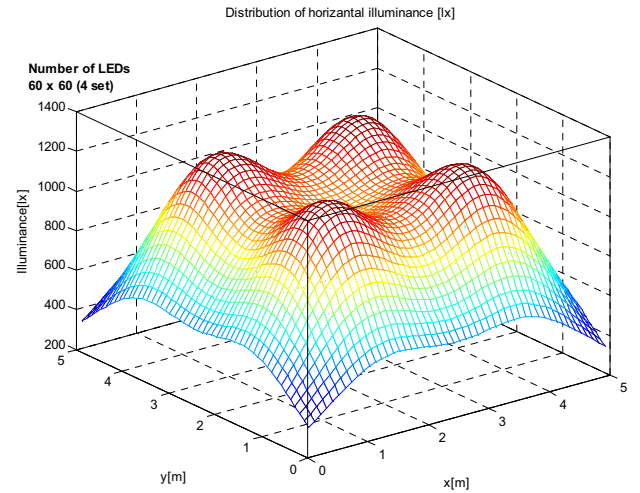


Fig 4. Distribution of illuminance for the simulation parameters.

the source beam,  $P_s$  is the total optical power and  $\phi = 0$  is the angle of maximum radiated power.

To provide sufficient lighting according to ISO, the illuminance must be between 300 to 1500 lx. All the simulation parameters adopted are listed in Table I. The distribution of illuminance is illustrated in Fig. 4, where the maximum and minimum values of illuminance are at 1210 lx and 334 lx, respectively.

Figure 5 depicted the predicted SER performance against the energy-to-noise ration ( $E_b/N_0$ ) for the BPSK, QPSK and 16-QAM modulation schemes for the LOS links showing a close match with the simulated data. Note that no pilot signal is used for the LOS links. The analytical OFDM system performance for M-QAM and QPSK modulation over AWGN channel is given by [24]:

$$P_{\sqrt{M}, QAM} = 2 \left( 1 - \frac{1}{\sqrt{M}} \right) Q \left( \sqrt{\frac{3}{M-1}} \frac{E_b}{N_0} \right) \quad (5)$$

$$P_{M, QAM} = 1 - \left( 1 - P_{\sqrt{M}} \right)^2, \quad P_b = P_M / \log_2^M$$

for QPSK

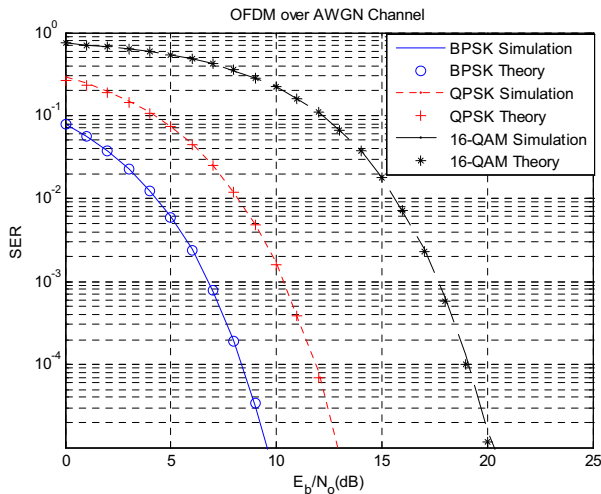


Fig 5. SER performance of LOS optical wireless OFDM link employing BPSK, QPSK and 16-QAM.

$$P_{\sqrt{M},QPSK} = 2P_{\sqrt{M},QAM}, P_{M,QPSK} = P_{M,QAM} / 2$$

and for BPSK over AWGN channel

$$P_b = \frac{1}{2} \operatorname{erfc} \left( \sqrt{\frac{E_b}{N_o}} \right). \quad (6)$$

The OFDM scheme employing the BPSK shows the best performance requiring 3.5 dB and 10.5 dB lower gains than QPSK and 16-QAM at the BER of  $10^{-4}$ , but at the cost of lower data rates.

Next we considered a diffuse channel with 16 taps (i.e.  $L = 16$ ). Since the number of data and pilot symbols is less than the subcarriers, we have used zero padding on both sides of the input symbols, which also provide immunity to the inter-symbol and inter-carrier interferences particularly at high data rates. Without loss of generality, we assumed the number of pilots is even which simplifies zero padding into the IFFT.

The channel impulse response in time domain is estimated by least-square error (LSE) as [20]:

$$\hat{h} = Gy \quad (7)$$

Where

$$G = (\varepsilon_p F_p D^H(X_p) D(X_p) F_p^H)^{-1} (\sqrt{\varepsilon_p} D(X_p) F_p^H)^H \quad (8)$$

and  $L \times N$  matrix  $[F]_{l,n} = \exp(j2\pi(l-1)(n-1)/N)$ ,  $\mathbf{f}_n$  is the  $n^{\text{th}}$  column of  $\mathbf{F}$  and  $L$  is the length of the channel,  $\mathbf{F}_p = [\mathbf{f}_{n1}, \dots, \mathbf{f}_{np}]$ ,  $H$  stand for the Hermitian transpose,  $D$  is a diagonal matrix and  $\varepsilon_p$  is the transmitted power per

pilot symbol. Having  $\hat{h}$  we can obtain the frequency response of the estimated channel on each subcarrier, which is used to equalize the received symbols. For the diffuse links we considered a frequency selective channel that has 16 zero-mean uncorrelated complex Gaussian random taps. Figure 6 illustrated the simulated symbol error rates (SER) versus the energy to noise ratio for OFDM system employing QPSK for a range of pilot symbols. As expected the performance improves when higher numbers of pilot symbols are used.

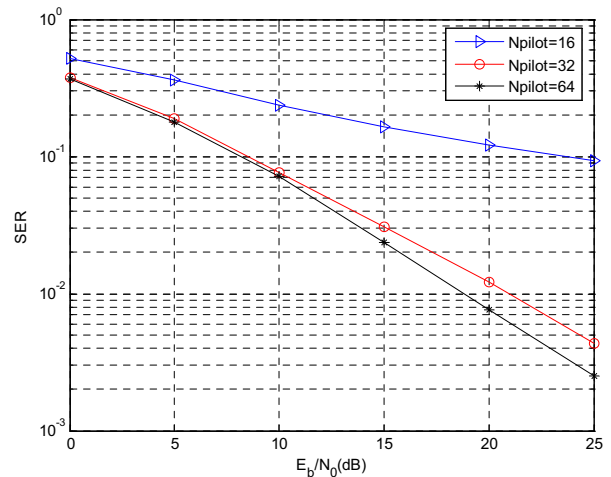


Fig 6. SER versus  $E_b/N_o$  for diffuse optical wireless OFDM link employing QPSK and LS channel estimation and for a number of pilot symbols.

### V. CONCLUSION

OFDM for indoor optical wireless communications (LOS and diffuse) using visible light LEDs have been presented. For diffuse links, pilot signals uniformly inserted into all symbols (subcarriers) were extracted at the receiver for channel estimation. The symbol error rate results for an OFDM employing BPSK, QPSK and M-QAM for LOS and diffuse links were presented for a range of pilot signal. It was shown that to achieve a lower SER high numbers of pilot signals will be need.

### REFERENCES

- [1] T. Komine, M. Nakagawa, "A Study of Shadowing on Indoor Visible-Light Wireless Communication Utilizing Plural White LED Lightings," *Int. Sympo. On Wireless Commun.*, pp. 36-40, 2004.
- [2] M.Z. Afgani, H. Haas, H. Elgala, D. Knipp, "Visible light communication using OFDM," *Proc. IEEE Symp. on Wireless Pervasive Computing*, TRIDENTCOM 2006.
- [3] T. Komine, M. Nakagawa, "Fundamental Analysis for Visible-Light Communication System using LED Lights," *IEEE Trans. on Consumer Electron.*, vol. 50, no., pp. 100-107, 2004.
- [4] M. Kavehrad, "Broadband room service by light," *Scint. American*, pp. 82-87, July 2007.
- [5] Z. Ghassemlooy, A.R. Hayes, and B. Wilson, "Reducing the effects of intersymbol interference in diffuse DPIM optical wireless communication", *IEE Proc. Optoelectron.*, vol. 150, no. 1, pp. 445-452, 2003.
- [6] K.K Wong,, T. O'Farrell, and M. Kiatweerasakul, "Infrared wireless communications using spread spectrum techniques," *IEE Proc., Optoelectron.*, vol. 147, no. 4, pp. 308-314, 2000.
- [7] J.B. Carruthers, and J.M. Kahn, "Angle diversity for nondirected wireless infrared communication," *IEEE Trans. Commun.*, vol. 48, no. 6, pp. 960-969, 2000.
- [8] T. Komine, L.J. Hwan, S. Haruyama, and M. Nakagawa, "Adaptive equalization for indoor visible-light wireless communication systems," *Asia-Pacific Conf. on Commun.*, pp. 294 - 298, 2005.
- [9] G. L. Stuber, J.R. Barry, S.W. McLaughlin, Ye Li M.A. Ingram, and T.G. Pratt, "Broadband MIMO-OFDM wireless communications," *IEEE Proc.*, vol. 92, no. 2, pp.271 - 294, 2004.

- [10] O. Gonzalez, R. Perez-Jimenez, S. Rodriguez, J. Rabadan, and A. Ayala, "Adaptive OFDM system for communications over the indoor wireless optical channel," *IEEE Proc. Optoelectron.*, vol. 153, no. 4, pp. 139-144, 2006.
- [11] J. R. Barry, J. M. Kahn, W. J. Krause, E. A. Lee, and D. G. Messerschmitt, "Simulation of multipath impulse response for indoor wireless optical channels," *IEEE J. Select. Areas Commun.*, vol. 11, no. 3, pp. 367-379, 1993.
- [12] Y. A. A and M. Kavehrad, "MIMO characterization of indoor wireless optical link using a diffuse-transmission configuration," *IEEE Trans. Commun.*, vol. 51, no. 9, pp. 1554-1560, 2003.
- [13] S. Rodríguez, R. Pérez-Jiménez, F. J. López-Hernández, O. González, and A. Ayala, "Reflection model for calculation of the impulse response on IR-wireless indoor channels using ray-tracing algorithm," *Microw. Opt. Technol. Lett.*, vol. 32, no. 4, pp. 296-300, 2002.
- [14] O. Gonzalez, S. Rodriguez, R. Perez-Jimenez, B.R. Mendoza and A. Ayala, "Error analysis of the simulated impulse response on indoor wireless optical channels using a Monte Carlo-based ray-tracing algorithm," *IEEE Trans. Commun.*, vol. 53, no. 1, pp. 124 - 130, 2005.
- [15] V. Pohl, V. Jungnickel, and C. von Helmolt, "Integrating sphere diffuser for wireless infrared communication," *Proc. Inst. Elect. Eng.-Optoelectron.*, vol. 147, no. 4, pp. 281-285, 2000.
- [16] V. Jungnickel, V. Pohl, S. Nönnig, and C. von Helmolt, "A Physical Model of the Wireless Infrared Communication Channel," *IEEE J. Select. Areas Commun.*, vol. 20, no. 3, pp. 631-640, 2002.
- [17] J. B. Carruthers and P. Kannan, "Iterative site-based modeling for wireless infrared channels," *IEEE Trans. on Ant. and Propag.* vol. 50, no. 5, pp. 759-765, 2002.
- [18] S. Colieri, M. Ergen, A. Puri, and A. Bahai, "Channel estimation techniques based on pilot arrangement in OFDM systems," *IEEE Trans. on Broadcast.*, vol. 48, no. 3., pp. 223-229, 2002.
- [19] S. Song and A.C. Singer, "Pilot-Aided OFDM channel estimation in the presence of the guard band," *IEEE Trans. Commun.*, vol. 55, no. 8, pp. 1459-1465, 2007.
- [20] X. Cai and G.B. Giannakis, "Error probability minimizing pilots for OFDM with M-PSK modulation over Rayleigh-fading channels," *IEEE Trans. Vehicular Tech.*, vol. 53, no. 1. pp. 146-155, 2004.
- [21] W. Zhang, X.-G. Xia, and P.C. Ching, "Optimal Training and Pilot Pattern Design for OFDM Systems in Rayleigh Fading," *IEEE Trans. on Broadcast*, vol. 52, no. 4, pp. 505-513, 2006.
- [22] J.H. Manton, "Optimal training sequences and pilot tones for OFDM systems," *IEEE. Commun. Letter*, vol. 5, no. 4, pp. 151-153, 2001.
- [23] J. Kim, J. Park, and D. Hong, "Performance analysis of channel estimation in OFDM systems," *IEEE Sig. Proc. Letters*, vol. 12, no. 1, pp. 60-62, 2005.
- [24] J.G. Proakis, M. Salehi, G. Bauch, "Contemporary communication systems using MATLAB and Simulink," 2nd ed. . - Belmont, CA; London : Thomson/Brooks/Cole, 2004.